Molecular Neurobiology (2019) 56:292–306
https://doi.org/10.1007/s12035-018-1045-5

Somatostatin Maintains Permeability and Integrity of Blood-Brain Barrier in β-Amyloid Induced Toxicity

Seungil Paik[1] · Rishi K. Somvanshi[1] · Ujendra Kumar[1]

Received: 10 August 2017 / Accepted: 27 March 2018 / Published online: 26 April 2018

Abstract

In Alzheimer's disease (AD), the impaired clearance of β-amyloid peptide (Aβ) due to disrupted tight junction and transporter proteins is the prominent cause of disease progression. Somatostatin (SST) blocks the aggregation of Aβ and inflammation whereas reduction of SST levels in the CSF and brain tissue is associated with impaired cognitive function and memory loss. However, the role of SST in preservation of blood-brain barrier (BBB) integrity and functionality in Aβ-induced toxicity is not known. In the present study using human CMEC/D3 cells, we demonstrate that SST prevents Aβ-induced BBB permeability by regulating LRP1 and RAGE expression and improving the disrupted tight junction proteins. Furthermore, SST abrogates Aβ-induced JNK phosphorylation and expression of MMP2. Taken together, results presented here suggest that SST might serve as a therapeutic intervention in AD via targeting multiple pathways responsible for neurotoxicity, impaired BBB function, and disease progression.

Keywords Alzheimer's disease · Blood-brain barrier · Somatostatin · Tight junction proteins and transporters

Introduction

Alzheimer's disease (AD) is a progressive neurodegenerative disorder and a common form of dementia characterized by the formation of neurofibrillary tangle, senile plaques, and the accumulation of β-amyloid peptide (Aβ) [1, 2]. The prominent cause of neuronal cell death in AD is associated with proteolytic cleavage of amyloid precursor protein along with excessive accumulation and aggregation of Aβ in the central nervous system (CNS). The activation of microglia and astrocytes has also been associated with neuronal loss in AD [3–5]. The release of pro-inflammation cytokines such as prostaglandins and matrix metallopeptidase (MMP) from brain microvessels in AD patients demonstrates the role of inflammation in the progression of AD. We have observed increased expression of astrocytes in close proximity of blood capillaries in AD patients [6]. In addition, a pro-inflammatory cytokine interleukin-1β (IL-1β) is increased in neuroinflammatory diseases and is associated with the impaired permeability of the blood-brain barrier (BBB). Previous studies have shown that defective clearance of Aβ from the brain in AD pathology is due to impaired BBB homeostasis. Normal brain homeostasis is prominently maintained by proper development and function of BBB. The main constituent of BBB is endothelial cells connected by tight- and adherens-junctions which exert a critical role in BBB permeability. The BBB maintains homeostasis of the CNS by regulating transportation of some molecules while restricting the permeability of others [7–10]. Moreover, such selective permeability of BBB is regulated by proper organization and expression of tight junction proteins (TJP), constituted with proteins such as ZO-1, ZO-2, occludin, and claudin [11–14]. By binding directly to other TJPs such as occludin and claudin, ZO-1 orchestrates the formation of tight junction complexes in BBB [15]. Previous studies have shown diminished levels of TJPs in the pathogenesis of AD [16, 17]. In addition, it has been noted that functional integrity of the BBB is crucial in the regulation of Aβ efflux and influx. In addition to the changes in the organization of TJPs, the Aβ efflux and influx through BBB are also regulated by low-density lipoprotein receptor-related protein (LRP) and the receptor for advanced glycation end products (RAGE). LRP exhibits high binding affinity to Aβ, whereas RAGE is crucial for neurite outgrowth, and also serves as a prominent receptor at BBB involved in regulation in the influx of peripheral and/or plasma Aβ [18]. The loss of LRP expression and increased RAGE activity has been reported in an age-dependent manner

✉ Ujendra Kumar
Ujendra.kumar@ubc.ca

[1] Faculty of Pharmaceutical Sciences, The University of British Columbia, V6T1Z3, Vancouver, BC, Canada

and believed to be a critical determinant of Aβ clearance and accumulation. The role of LRP in Aβ clearance is further supported by studies in LRP1 *ko* mice displaying over-accumulation of Aβ [19]. Furthermore, the functional relation between RAGE and TJPs is also reported in AD model [20].

MMPs are a family of proteases involved in various physiological functions including cleavage of zymogens, activation of growth hormones, and remodeling of extracellular matrix (ECM). Specifically, the remodeling of ECM by MMPs has been studied extensively for its potential implication in cognitive impairment as evident in various neurodegenerative diseases. Furthermore, MMPs have been reported to break down TJPs forming BBB, leading to hemorrhage. Among the family of MMPs, MMP2 and 9 have been studied extensively for their involvement in ECM disruptions. MMPs via many proteolytic reactions have been associated with several cell surface entities including receptors and junction proteins [21]. Moreover, previous studies have emphasized the role of MMPs in TJPs and impaired BBB permeability [22]. The degradation of occludin and claudin has also been reported in response to MMPs [23].

Somatostatin (SST), a growth hormone inhibitory peptide widely expressed in central and peripheral tissues, exerts a variety of endocrine and non-endocrine functions. In addition to a neuroprotective role in excitotoxicity, decreased level of SST has been reported in several neurological diseases [24–29]. Furthermore, the cortical and cerebrospinal fluid (CSF) levels of immuno-reactive SST are markedly decreased in AD and have become reproducible biochemical marker of the disease [30]. We have shown changes in SST secretion and accumulation in cultured cortical neurons in response to Aβ-induced neurotoxicity and expression of SST receptors (SSTRs) in AD brain tissue [6, 31]. SST increases neprilysin, an enzyme involved in degradation of Aβ, and SST *ko* mice exhibit decreased neprilysin and increased Aβ deposit [32].

We previously demonstrated changes in the expression of SSTR subtypes as well as modulation of cytokine and SST release in the human cerebral microvascular endothelial cell line (hCMEC/D3) in response to lipopolysaccharide (LPS) treatment. Moreover, the same study also supports the role of SST in the organization of TJP surface expression perturbed in the presence of LPS and cytokines [33]. Furthermore, another study reported that *Sstr2*$^{-/-}$ mice showed selective degeneration of their central noradrenergic projections, suggesting the role of specific SST receptors in progression of AD [34]. It is unknown whether SST is involved in the regulation of Aβ influx or efflux and permeability of BBB. In the present study, using a combination of morphological, biochemical, and molecular approaches, we aimed to investigate the role of SST in protection against Aβ-induced damage in hCMEC/D3 cells. Here, we demonstrate that the presence of SST protects BBB integrity by maintaining the organization of TJPs against Aβ-induced damage.

Material and Methods

Materials

The human brain microvascular endothelial cell line (hCMEC/D3) was a kind gift from Dr. P.O. Couraud (Institut Cochin, INSERM, CNRS, Université Paris Descartes, Paris, France). Endothelial basal medium-2 (EBM-2) was purchased from Lonza (Basel, Switzerland). The culture medium was purchased from Thermo Fisher Scientific (Massachusetts, USA) and was supplemented with ascorbic acid and lipid concentrate. HEPES, basic fibroblast growth factor (bFGF), and hydrocortisone were obtained from Sigma-Aldrich Inc. (St. Louis, MO, USA). SST-14 was purchased from Bachem (Torrance, CA, USA). Aβ-peptides were purchased from EZ Biolab (Westfield, IN, USA), and the scrambled Aβ-peptide was purchased from Anaspec (Fremont, CA, USA). All other reagents were of analytical grade and purchased from various sources.

Cell Culture

hCMEC/D3 cells were cultured and maintained as previously described [33]. Briefly, the cells were cultured and maintained in flasks or culture dishes precoated with rat tail collagen-I and grown until complete confluence in all experimental setup. The EBM-2 media was supplemented with 5% fetal bovine serum (FBS), 1% penicillin-streptomycin, 5 μg/mL ascorbic acid (AC), 1.4 μM hydrocortisone (HC), 10 mM HEPES, 1 ng/mL bFGF, and chemically defined lipid concentrate at 1:100 dilution. All experiments were carried out using cells within passages 27–33.

MTT Assay

Cells were treated with increasing concentration of Aβ for 24 h and were processed for MTT assay. Briefly, 300 μg/mL of methylthiazolyldiphenyl-tetrazolium bromide solution (Sigma) was prepared in DMEM. Following dose-dependent treatment with Aβ1-42 (0, 1, 5, 25 μM) for 24 h, hCMEC/D3 cells were incubated with prepared MTT solution for 3 h at 37 °C. Following subsequent washes with PBS, 100 μL of isopropanol was added to each well, and the resulting change in color from dissolving formazan salt was immediately quantified using spectrophotometer at a wavelength of 550 nm with background absorbance measured at 695 nm. Results are presented as a percentage of control versus treated group.

Caspase/Apoptosis Activity Assay

The apoptosis in hCMEC/D3 cells treated with Aβ1-42 in presence or absence of SST was assessed using Caspase-3/7

Green Apoptosis Assay (Essen Bioscience, Michigan, USA) following manufacturer's instructions. Briefly, cells were treated with Aβ1-42 (5 μM) alone or in combination with increasing concentrations of SST (1 nM, 100 nM, 1 μM) in presence of a DNA intercalating dye NucView™488 (Essen Bioscience). Immediately after treatments, the plate was placed in live-cell imaging system (Essen Bioscience) and caspase-3/7 activity was monitored up to 48 h as an index of cells undergoing apoptosis and calculated using IncuCyte basic analyzer (Essen Bioscience).

Live/Dead Cell Assay

The cell viability upon treatments with Aβ1-42 in the presence or absence of SST was analyzed using LIVE/DEAD Cell Vitality Assay (Thermo Fisher Scientific) following manufacturer's instructions. Briefly, the cells were treated with Aβ1-42 (5 μM) alone or in combination with SST (1, 30, 100, 300, 1000 nM) for 24 h. Following treatment, cells were washed with PBS and collected using 0.05% trypsin-EDTA (Thermo Fisher Scientific). Trypsinized cells were then re-suspended in 100 μL of PBS and incubated with C_{12}-resazurin (20 ng/μL) and SYTOX dye (1 μM) for 15 min at 37 °C. A total of 400 μL of PBS was then added to make total suspension of 500 μL, and the cells were immediately analyzed on LSR II (BD Bioscience, CA, USA) with fluorescence excitation at 488 nm and emission at 530 and 570 nm. All resulting data was analyzed using FlowJo workstation (BD bioscience).

Western Blotting

To determine time and dose-dependent effect of Aβ on protein expression, hCMEC/D3 cells were treated with two concentrations of Aβ (1 and 5 μM) for 2 and 6 h. In addition, the dose-dependent effect of Aβ (200 nM, 1 μM, 5 μM) with or without increasing concentration of SST (400 nM, 2 μM, 10 μM) was further assessed for 24 h at 37 °C. Post-treatment, cells were lysed using RIPA (radio-immune precipitation assay) buffer supplemented with phosphatase and protease-inhibitor (1:100). Total protein content was measured by Bradford Protein Assay (Biorad, Hercules, California, USA). A total of 15 μg of protein per sample was fractionated on SDS-PAGE gel and transferred to nitrocellulose membrane. The membranes were incubated with mouse monoclonal-ZO-1 (1:500, Abcam, Cambridge, UK), rabbit polyclonal-Occludin (1:1000, Thermo Fisher Scientific, Waltham, Massachusetts, USA), rabbit monoclonal-LRP1 (1:1000, Abcam), rabbit monoclonal-RAGE (1:1000, Abcam), mouse monoclonal-pJNK and -total JNK (1:1000, Santa Cruz Biotechnology, Dallas, TX, USA), and rabbit polyclonal-MMP2 (1:1000, Abcam) primary antibodies overnight at 4 °C. The membranes were washed and incubated with species-specific, HRP-conjugated secondary antibodies (1:2000, Jackson ImmunoResearch, West Grove, PA, USA) and developed using enhanced chemiluminescence detection kit (Millipore, Billerica, MA, USA) on Alpha Innotech FluorChem 8800. β-actin was used as internal control. Densitometric analysis of immunoblot was performed using ImageJ software (US National Institutes of Health, Bethesda, Maryland, USA).

Enzyme-Linked Immunosorbent Assay

For the detection of SST and IL-1β release, ELISA analysis was performed following manufacturers' instruction. Briefly, culture media from control and treated cells were collected and added to 96-well plate pre-coated with SST or IL-1β antibody and incubated for 1 to 2 h, respectively (SST, Cloud-Clone Corp, TX, USA and IL-1β, BD Bioscience). The plate was then incubated with provided detection reagent for 1 h at 37 °C for SST and 30 min for IL-1β at room temperature (RT). Subsequently, the plates were incubated for 30 min at 37 °C in 100 μL of detection reagent B or enzyme working reagent for SST and IL-1β, respectively. The substrate was added for respective kits and the incubation was terminated by adding 50 μL of Stop Solution to each well. The absorbance was read at 450 nm using spectrophotometer (BMG Labtech, Germany). Data were quantified and analyzed as per manufacturer's instructions.

Immunofluorescence Staining

hCMEC/D3 cells were grown to confluence on glass coverslip pre-coated with rat tail collagen I. Cells were treated with Aβ (5 μM), SST (2 μM) alone, or in combination for 24 h. Following treatment, control and treated cells were fixed with 4% paraformaldehyde at 4 °C for 15 min. Cells were permeabilized with 0.1% Triton-X solution for 15 min at RT, washed with PBS, and incubated in 5% normal goat serum (NGS) for 1 h at RT. Cells were then incubated with primary antibodies, ZO-1 (1:200), Occludin (1:150), LRP1 (1:150), RAGE (1:150) in TBS containing 5% NGS overnight at 4 °C. Following wash, cells were incubated for 1 h at RT with Alexa-594 tagged secondary antibody (1:200). To visualize the nucleus, cells were exposed to Hoechst 33258 dye (0.5 μg/mL, Calbiochem, CA, USA) for 10 min at RT. Coverslips were then mounted on slides and photographed using Zeiss LSM700 confocal microscope (Carl Zeiss, Germany).

Permeability Assay

hCMEC/D3 cells were grown to confluence on 0.4 μM pore-transwell inserts (Greiner bio-one, Austria) pre-coated with rat tail collagen-I. The cells were treated with either increasing

concentration of Aβ (1, 5, 25 μM) and SST (80 nM, 400 nM, 2 μM, 10 μM) alone or in combination (Aβ: 5 μM, SST: 80 nM, 400 nM, 2 μM, 10 μM) for 24 h. The paracellular permeability of hCMEC/D3 cells to FITC-dextran (40 kD, Sigma Aldrich, St. Louis, MO, USA) was then quantified as previously described [35]. Briefly, 2 mg/mL of 40 kDa FITC-dextran was loaded onto apical chamber of transwell insert for 30 min at 37 °C. To determine the amount of FITC-dextran that passed through, 100 μl of media from the basolateral chamber was collected and the fluorescence intensity (FITC-dextran excitation wavelength 495 nm, emission 519 nm) was measured using spectrophotometer (BMG Labtech, Germany).

Cellular Uptake and Efflux Quantification

The quantification of Aβ influx and efflux in hCMEC/D3 cells was determined as previously described [36]. Briefly, for the quantification of Aβ uptake (influx), hCMEC/D3 cells were cultured until 100% confluency. Cells were washed twice with PBS and incubated with either fluorescein (FAM)-Aβ1-42 (100 nM) alone, in combination with SST (2 μM), or 15 min pre-treatment of cells with SST (2 μM) followed by FAM-Aβ1-42 (100 nM) for 30 min at 37 °C. Following treatment, cells were washed with PBS and enzymatically detached using 0.05% Trypsin (Thermo Fisher Scientific). The cells were resuspended in PBS, washed, and fixed in 4% paraformaldehyde for 10 min. Fixed cells were then washed in PBS, centrifuged, and re-suspended in FACS solution (PBS containing 2% FBS and 2 mM EDTA) for analysis. The cells were analyzed in LSR II (BD Bioscience) using Blue laser excitation at 488 nm.

For efflux study, hCMEC/D3 cells were plated and treated as described above for 10 min at 37 °C. The media was removed, and the cells were washed three times with PBS to remove residual FAM-Aβ1-42. Media was then replaced with FAM-Aβ1-42 free medium, and cells were incubated for an additional 20 min. The cells were then processed and analyzed as described above. All resulting data was analyzed using FlowJo workstation.

Statistical Analysis

All experimental data are presented as mean ± SEM of minimum three independent experiments. All statistical analysis was performed using GraphPad Prism 5. For analysis of data with one independent variable in more than two groups, one-way analysis of variance (ANOVA) was used. For data with one independent variable in two groups, two-tailed unpaired Student's *t* test was performed as indicated. In all cases, *p* value less than 0.05 was considered significant.

Results

Concentration-Dependent Effect of Aβ1-42-Induced Toxicity in hCMEC/D3 Cells

To establish Aβ-induced toxicity models, we first determined the concentration-dependent effect of Aβ on hCMEC/D3 cell survival. At lower concentrations, Aβ1-42 (5, 10 μM) had no significant effect on cell viability; however, at relatively higher concentrations (25 μM), Aβ exhibited 50% cell death (Fig. 1a). In support of MTT assay, Hoechst nuclear staining was performed to visualize changes in cells treated with Aβ1-42 (Fig. 1b).

Previous reports have indicated that Aβ1-42-induced toxicity is mediated via apoptotic pathway [37]. To further elucidate and establish the correlation between Aβ1-42 and apoptosis, hCMEC/D3 cells treated with Aβ1-42 (5 μM) alone or in combination with SST in dose-dependent manner were incubated with caspase-specific NucView™488. Cells were monitored up to 48 h to assess caspase-3/7 activation following treatment. In the presence of Aβ1-42 alone, caspase-3/7 activity showed a gradual, time-dependent increase (Fig. 1c). In contrast, the untreated control and cells treated with SST (1 μM) alone displayed minimal changes in caspase-3/7 activity. Cells treated with Aβ1-42 in the presence of increasing concentrations of SST showed significantly lower caspase-3/7 activity when compared to the cells treated with Aβ1-42 alone, indicating an inhibitory effect of SST on caspase-activity in hCMEC/D3 cells.

To further elucidate and support our results from caspase-3/7 activity, we next investigated the cell viability using LIVE/DEAD Cell Vitality Assay. By assessing the reduction of C_{12}-resazurin in metabolic cells as well as inclusion of impermeable SYTOX dye, the LIVE/DEAD Cell Vitality Assay allowed accurate quantification of cell viability. In alignment with caspase-3/7 activity results, cells treated with Aβ1-42 alone showed increase in FITC positive cells, indicating increased cell permeability of cells and apoptosis/toxicity compared to untreated control (Fig. 1d, e). In contrast, the cells treated with SST alone showed comparable number of FITC positive cells with untreated control. In parallel with caspase activity, cells treated with Aβ1-42 in combination with increasing concentrations of SST showed a dose-dependent decrease in FITC positive cells, suggesting a protective role of SST against Aβ1-42-induced toxicity. Taken together, results obtained from caspase activity and live/dead cell viability assay suggesting a protective role of SST in Aβ-induced toxicity.

Aβ1-42-Induced Release of IL-1β in hCMEC/D3 Cells Is Blocked in Presence of SST

To investigate the cytokine release, hCMEC/D3 cells grown to confluency were treated with Aβ1-42 (5 μM) in absence or presence of SST (2 μM) for 24 h at 37 °C. Post-treatment

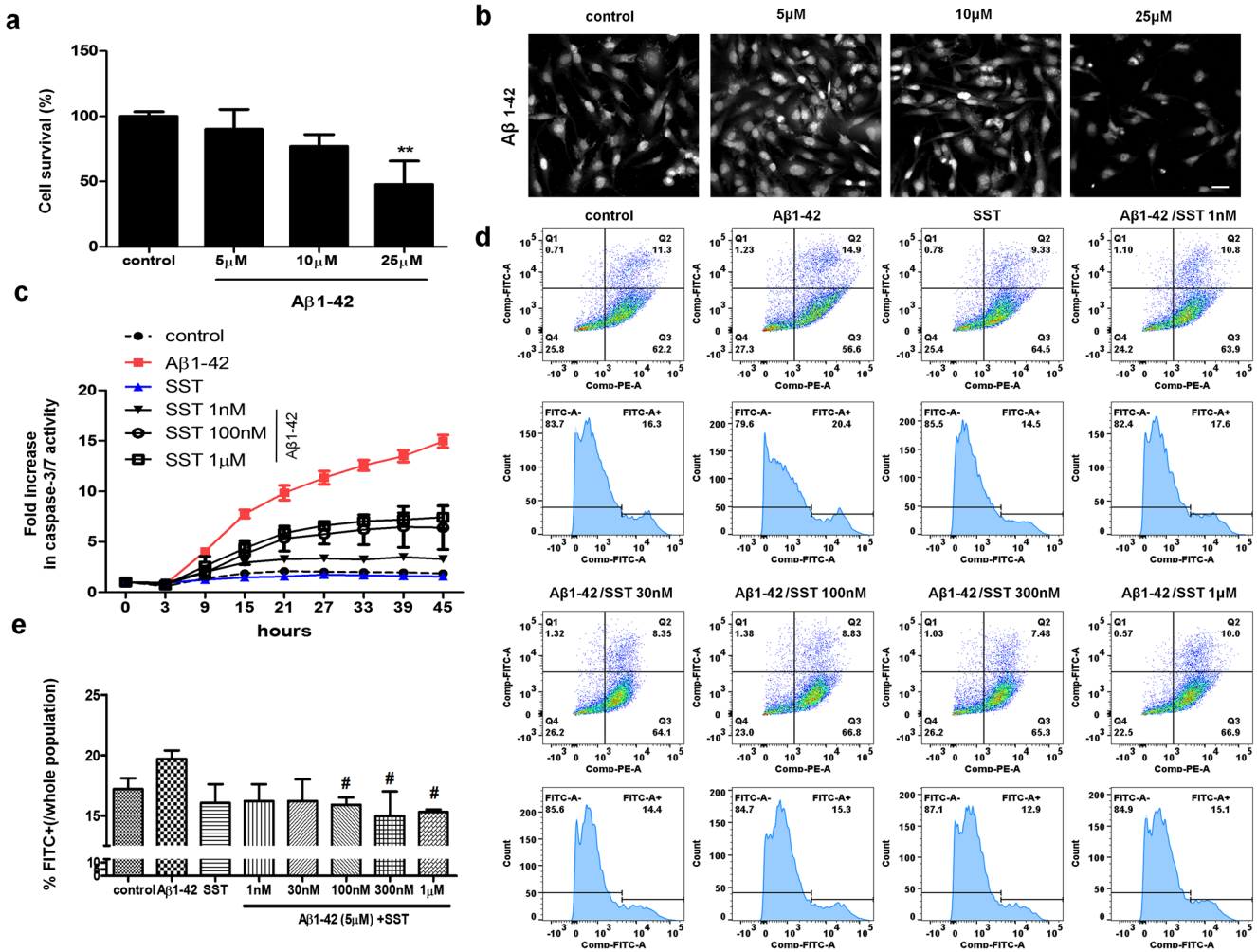

Fig. 1 SST inhibits Aβ-induced toxicity in hCMEC/D3 cells. **a** hCMEC/D3 cells were treated with increasing concentration of Aβ1-42 (5–25 μM) for 24 h at 37 °C and processed for MTT assay. Aβ-induced cell death in dose-dependent manner. **b** Hoechst staining of hCMEC/D3 cells treated with increasing concentration of Aβ1-42 shows dose-dependent toxicity. **c** SST inhibits Aβ1-42-induced caspase-3/7 activation. Cells co-treated with Aβ1-42 and SST shows significant inhibition of caspase-3/7 activity. **d** Dot plot data of C_{12}-resazurin and SYTOX fluorescence intensity (dot plot) and FITC intensity distribution (histogram) displays distribution of cells based on viability. FITC positive cells on histogram represent dead cells with higher SYTOX inclusions. **e** SYTOX cell permeability assay indicates significant increase in permeability in cells treated with Aβ1-42 (5 μM) alone, whereas dose-dependent inhibition in presence of increasing concentrations of SST. $^{**}p < 0.01$ against control, $^{\#}p < 0.05$ against Aβ1-42 treated alone. *Scale bar* = 20 μm

culture medium was collected and processed for IL-1β quantification using ELISA according to manufacturer's instructions. The IL-1β release was approximately fourfold higher upon treatment with Aβ1-42 in comparison to control (Fig. 2a). Augmented IL-1β release in response to Aβ1-42 was suppressed significantly in the presence of SST and was comparable to SST treatment alone.

Release of SST Is Unaffected in Response to Aβ1-42

In addition to the decreased levels of SST in CSF of AD patients, previous studies using neuronal culture and hCMEC/D3 cells have shown changes in SST release in response to Aβ1-42 and LPS treatment [31]. To address whether Aβ is involved in regulation of SST release, hCMEC/D3 cells were treated with increasing concentration of Aβ (400 nM, 2 μM, 10 μM) for 24 h. Post-treatment, culture medium was collected and processed to determine SST content by ELISA according to manufacturer's instruction. SST release in response to Aβ remained comparable to control, although a decreasing trend in SST release was observed with increasing concentrations of Aβ1–42 (Fig. 2b).

Concentration and Time-Dependent Effect of Aβ1-42 on TJP Expression in hCMEC/D3 Cells

The release of cytokines from hCMEC/D3 cells in response to Aβ1-42 is an indication of inflammation and impaired cell permeability. Consistent with previous studies demonstrating that TJPs are crucial for BBB integrity, we next explored

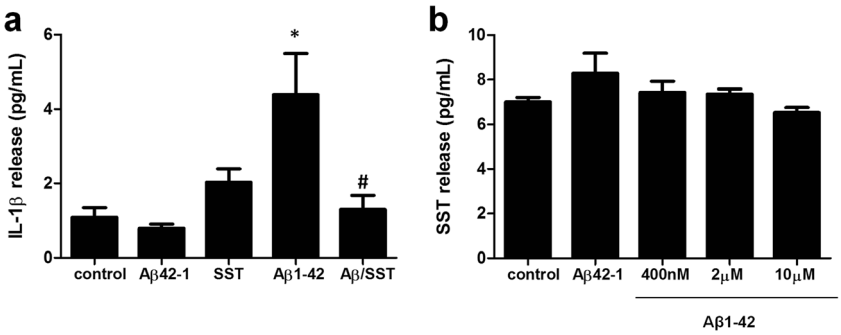

Fig. 2 Aβ1-42-induced cytokine release in hCMEC/D3 cells. **a** Pro-inflammatory cytokine IL-1β release was significantly increased in presence of Aβ (5 μM), which was inhibited in presence of SST. **b** SST release was not changed in presence of Aβ as indicated ($n = 3$). *$p < 0.05$ against control

whether Aβ1-42-induced toxicity and/or IL-1β release is associated with the disruption of TJP expression in cells. To address this, we first determined the expression of ZO-1 and occludin in control and cells subjected to Aβ treatment in a concentration- and time-dependent manner. hCMEC/D3 cells grown to confluency were exposed to Aβ1-42 (1 and 5 μM) for 2 and 6 h at 37 °C (Fig. 3). Cell lysates prepared from control and treated cells were immunoblotted for the expression of ZO-1 and occludin. The expression level of both ZO-1 and occludin was decreased significantly in cells treated with Aβ in concentration- and time-dependent manner (Fig. 3a). Unlike ZO-1, occludin showed rapid recovery of expression at a lower concentration of Aβ1-42 (1 μM) treatment, while under the higher concentration of Aβ1-42 (5 μM), the expression remained inhibited.

Concentration- and Time-Dependent Effect of Aβ1-42 on LRP1 and RAGE in hCMEC/D3 Cells

Along with para-cellular integrity maintained by ZO-1 and occludin, various transporters play a pivotal role in the trans-cellular transportation of Aβ across BBB [38]. To delineate whether the loss in TJP expression is also linked to abnormal efflux and/or influx in hCMEC/D3 cells, we first attempted to determine the expression level of LRP1 and RAGE in cell lysate prepared from hCMEC/D3 cells following treatment with Aβ1-42 in concentration- and time-dependent manner. LRP1 and RAGE expression levels were significantly decreased upon treatment with Aβ in time- and dose-dependent manner (Fig. 3b). Similar to occludin, RAGE showed significant recovery following 6 h post-treatment with

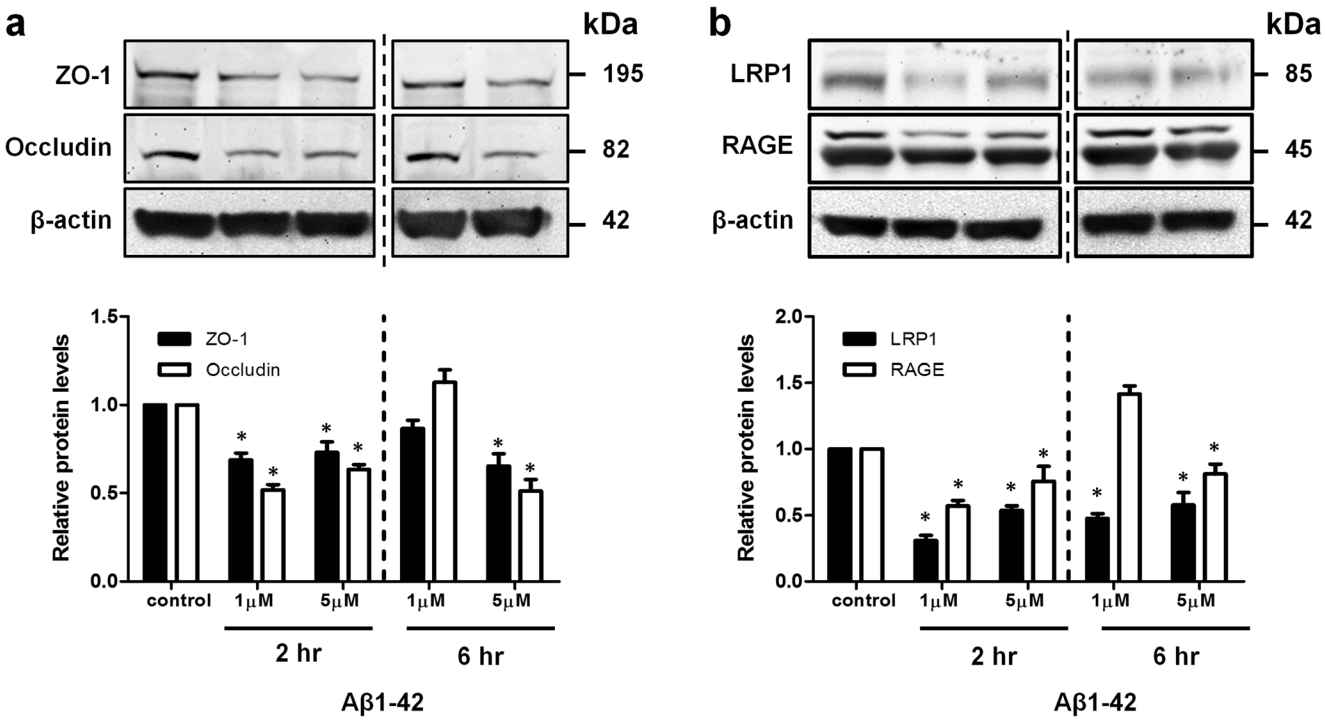

Fig. 3 Aβ modulates TJPs and Aβ transporter expression in time- and dose-dependent manner. **a** Representative Western blot showing decreased level of ZO-1 and occludin (upper panel). Histograms represent densitometric analysis of Western blot (bottom panel). **b** Representative immunoblot analysis (upper panel) and densitometric analysis of Western blot (bottom panel) show decreased level of Aβ transporters LRP1 and RAGE. Note significant recovery of RAGE at a lower concentration with prolonged treatment (6 h). β-actin was used as loading control. Data represents mean ± SEM of three independent experiments. *$p < 0.05$ against control

a lower concentration of Aβ1-42 (1 μM). These results suggest transient changes in transporter proteins, which tend to return to the normal depending on intensity and duration of insult.

Exogenous SST Improved Aβ-Induced Disruption of TJPs in BBB

In order to assess whether SST restores Aβ-induced disruption of ZO-1 and occludin expression levels at the cell surface, cells were treated with Aβ in the presence of increasing concentration of SST (400 nM–10 μM) for 24 h. Scrambled Aβ was used as negative control. Post-treatment, cells were processed for subcellular distribution and expression of ZO-1 and occludin using immunofluorescence immunocytochemistry and Western blot analysis. The distributional pattern of ZO-1 immunostaining in the presence of SST alone was comparable to control group (Fig. 4a). However, ZO-1 immunostaining at the cell surface displayed discontinuation in the expression in cells treated with Aβ. Interestingly, the treatment of cells with SST in combination with Aβ resulted in an intact and continuous expression pattern of ZO-1 immunoreactivity at the cell-cell interface that was comparable to the control or cells treated with SST (Fig. 4a). Western blot was performed to determine whether SST restores ZO-1 immunoreactivity at the cell surface as well as the expression of ZO-1 in presence of Aβ. Immunoblot analysis revealed dose-dependent decrease in ZO-1 expression upon treatment with Aβ (Fig. 4c). Such decreased ZO-1 expression was recovered to the control level in presence of SST at lower concentrations (400 nM and 2 μM). However, at higher concentration, SST had no effect on ZO-1 expression.

We next determined the distributional pattern and expression of occludin in similar experimental conditions as described for ZO-1. No significant changes were seen in the distribution of occludin immunoreactivity at cell surface upon treatments as indicated (Fig. 4b). The expression level of occludin was increased in all treatment conditions excluding 400 nM SST in presence of 5 μM of Aβ (Fig. 4c). However, SST treatment alone (2 μM) also resulted in increased expression of occludin when compared with control. Taken into consideration, the results described here delineate that lower concentration of SST can normalize Aβ1-42-induced disruption in TJP organization and its expression.

SST-Mediated Protection Against Aβ-Induced Toxicity Modulate LRP1 and RAGE Expression and Activity

Aβ clearance from the brain to CSF and its influx to the neurons from peripheral tissues via circulation is mediated by two prominent receptors protein, LRP1 and RAGE, respectively [38, 39]. Previous studies have also demonstrated decreased expression of LRP1 in contrast to increased expression of RAGE in AD brain; however, the role SST might play in regulation of LRP1 and RAGE is not well understood. Both LRP1 and RAGE were not significantly changed in subcellular distribution of immunofluorescence staining (Fig. 5a). However, immunoblot revealed that the basal expression of LRP1 in cell lysate was down-regulated in comparison to control when cells were treated with SST (2 μM) alone (Fig. 5b). In addition, LRP1 expression was significantly increased when Aβ was used in combination with SST. Western blot analysis also revealed upregulation of RAGE expression in cell lysate prepared from Aβ-treated cells. Such enhanced expression of RAGE was down-regulated to the basal level in presence of SST when used in combination with Aβ (Fig. 5b). The suppression of RAGE expression in the presence of SST alone and in combination with Aβ was significantly lower than control.

Impaired Cell Permeability with Aβ Is Improved with the Use of SST

Transwell permeability assay was performed to determine whether the perturbed organization of ZO-1 and occludin along with changes in expression of LRP1 and RAGE are directly associated with cell permeability (Fig. 6a). Increased level of FITC-dextran was observed in the basolateral chamber in response to Aβ in a concentration-dependent manner due to enhanced cell permeability (Fig. 6b). To assess the effect of SST on BBB permeability, cells were then treated with increasing concentration of SST (80 nM–10 μM). Increasing concentration of SST exhibits decreased FITC-dextran levels in the basolateral chamber when compared with control, scrambled, and Aβ treatment (Fig. 6c). In order to assess whether the presence of SST block Aβ-mediated increase in permeability, cells were treated with Aβ alone and in combination with different concentration of SST (80 nM–10 μM) for 24 h. SST displayed inhibition of FITC-dextran permeability in the basolateral chamber in comparison to control and/or Aβ-treated cells (Fig. 6d). Scrambled Aβ was used as a negative control. Collectively, these results suggest that SST provide protection against Aβ1-42-induced damage to BBB permeability either directly or indirectly through improving the expression of TJP and/or limiting the active influx of Aβ by inhibiting Aβ-binding to transporters such as LRP1 and RAGE.

Pretreatment with SST Affects Aβ1-42 Influx and Efflux in hCMEC/D3 Cells

To investigate whether changes in cell permeability are linked to impaired efflux and influx of Aβ in cells, FACS analysis was used to determine the influx/efflux of FAM-dye conjugated Aβ in hCMEC/D3 cells with or without SST. Fluorescently labeled Aβ (FAM-Aβ1-42) was used to treat confluent

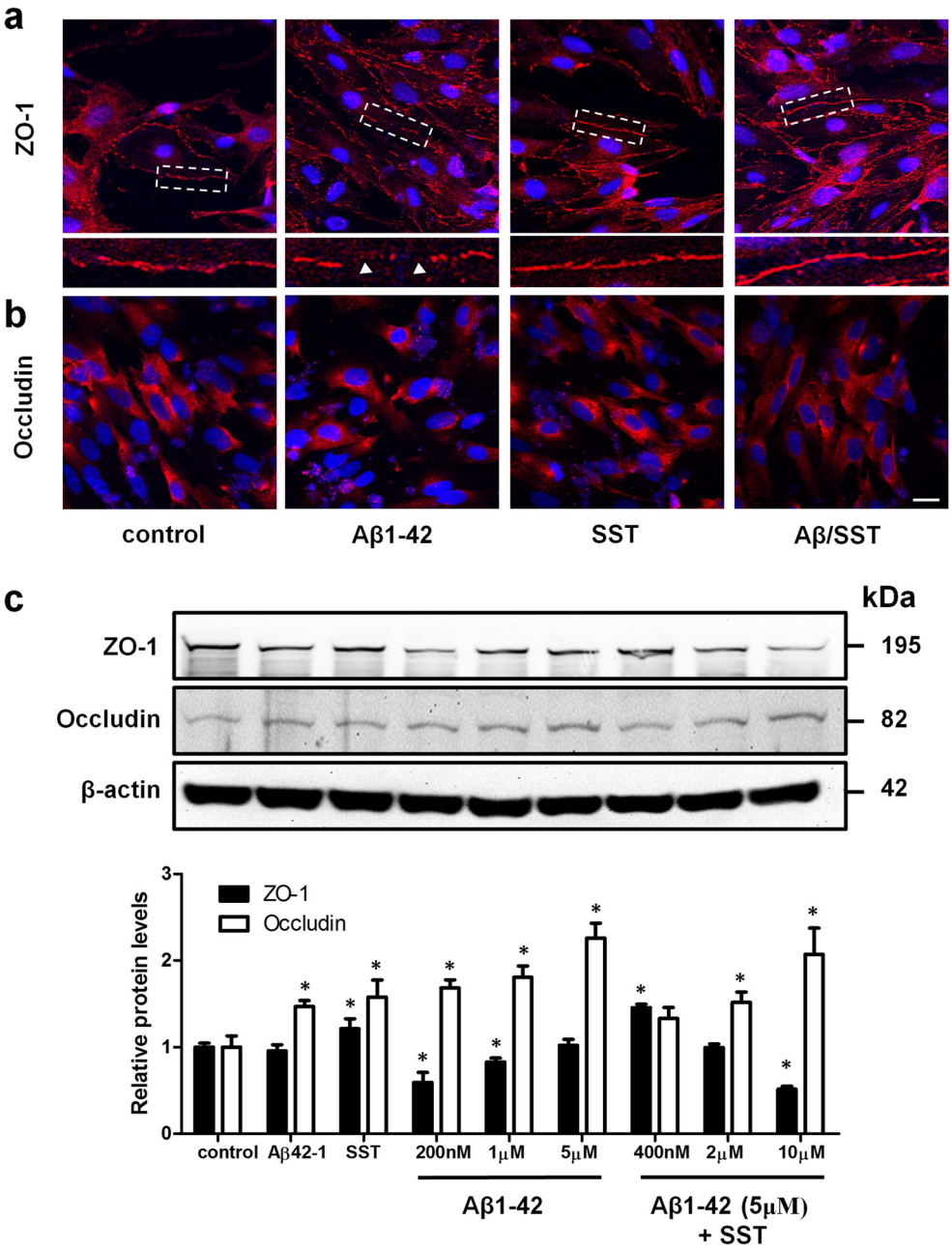

Fig. 4 SST inhibits Aβ-induced damage on TJP integrity and expression. **a** Immunofluorescence staining of ZO-1 and occludin. Control hCMEC/D3 cells exhibited continuous staining of ZO-1 on cell periphery, whereas Aβ-induced discontinuation in ZO-1 staining as indicated by fragmented staining. Note the normal staining of ZO-1 in presence of SST alone and restoration of ZO-1 like immunoreactivity at cell surface when used in combination with Aβ. High magnification of selected area at cell membrane displayed pattern of ZO-1 disturbance (arrowhead). **b** Occludin immunofluorescence was not changed upon treatment as indicated. **c** Representative Western blot depicts changes in ZO-1 and occludin expression following dose-dependent treatment with either Aβ alone or in presence of increasing concentration of SST as indicated. Densitometry analysis revealed the opposing effect of Aβ on ZO-1 and occludin expression, which was significantly inhibited in presence of SST. β-actin was used as a loading control. $*p < 0.05$ against control. *Scale bar* = 20 μm

hCMEC/D3 cells, and the uptake was monitored through the bright field and fluorescence microscopy (Fig. 7a) and immunostaining with phalloidin (Fig. 7b). In both preliminary assessments, we observed significant uptake of FAM-Aβ1-42 by cells as early as 10 min post-treatment. FACS analysis was performed to quantify the amount of FAM-Aβ1-42 inside the cells following each treatment as indicated. Briefly, the cells were treated with either FAM-Aβ1-42 alone and in combination with SST, or incubated with SST for 15 min prior to the addition of FAM-Aβ1-42 and processed for the influx of Aβ (Fig. 7c, upper panel) and efflux (Fig. 7c, bottom panel). To determine the Aβ influx, the geometric fluorescence mean intensity (GMFI) was measured following 30 min of treatment. Aβ influx was not significantly changed in cells treated with Aβ alone or in combination with SST (Fig. 7d). However, cells pre-treated with SST (SST + Aβ) for 15 min before the addition of Aβ resulted in significant inhibition of influx (Fig. 7d). We next determined Aβ efflux under similar treatment conditions as described for the influx. As seen in influx, in cells co-treated with FAM-Aβ1-42 and SST, the GMFI was similar to FAM-Aβ1-42 alone. However, when the hCMEC/D3 was pre-incubated with SST for 15 min prior to the addition of FAM-Aβ1-42, there was a significant decrease in GMFI (Fig. 7e). These data suggest that the presence of SST effectively inhibit the Aβ uptake by hCMEC/D3 cells.

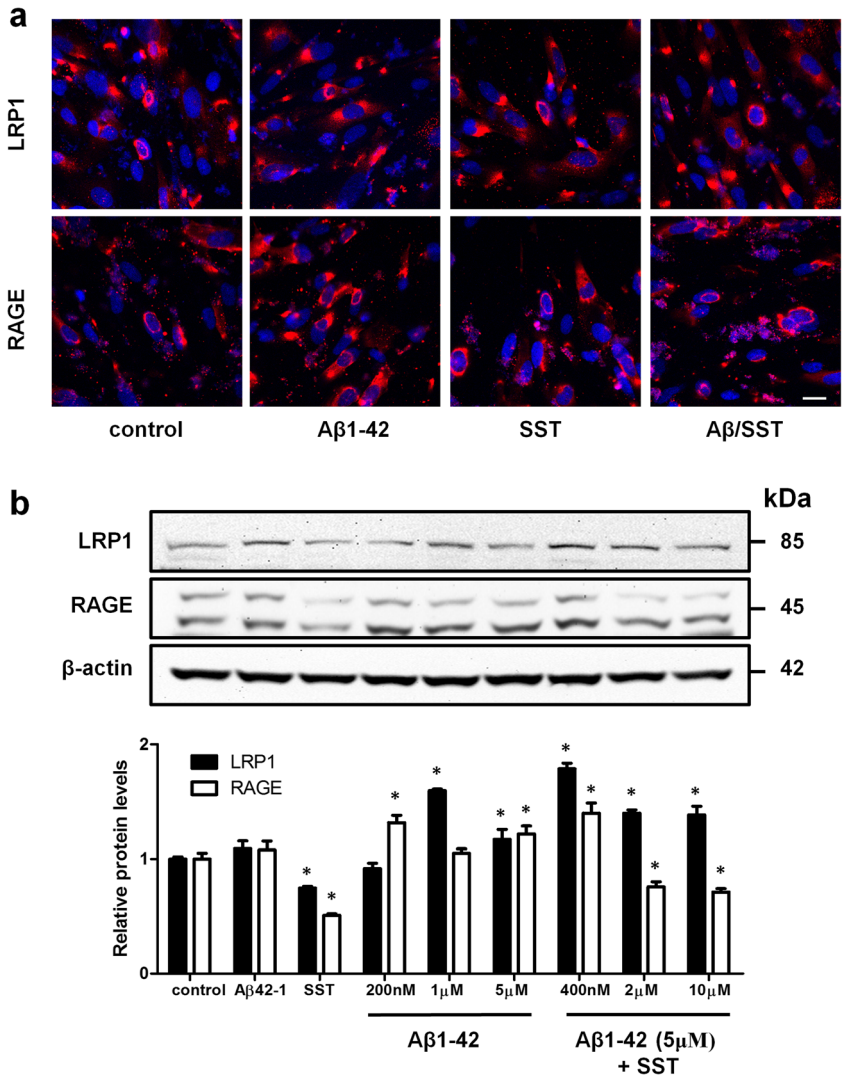

Fig. 5 SST restores Aβ-induced changes on Aβ1-42 transporter protein expression. **a** Subcellular distributional pattern of both LRP (upper panel) and RAGE (lower panel) was not visibly affected by the presence of Aβ or SST. **b** Western blot analysis revealed concentration-dependent changes in expression of LRP1 and RAGE in presence of Aβ alone. Note the significant inhibition of Aβ-mediated changes in presence of SST. Histograms indicate that the presence of SST increased the expression of LRP1 while reducing the expression of RAGE. β-actin was used as a loading control. $*p < 0.05$ against control. *Scale bar* = 20 μm

Role of SST in Regulation Aβ-Mediated Changes in JNK Phosphorylation and MMP2 Expression in hCMEC/D3 Cells

To dissect out the possible mechanism of Aβ-mediated disruption of BBB, the status of JNK expression and phosphorylation and expression of MMP2 was determined in hCMEC/D3 cells following treatment with Aβ in presence or absence of SST. SST and Aβ-scramble displayed no significant effect on JNK activation. Phosphorylation of JNK was significantly enhanced in the presence of Aβ (200 nM), whereas decreasing trend of JNK activation was observed with Aβ treatment in a dose-dependent manner. In contrast, SST treatment in presence of Aβ displayed inhibition of JNK expression and was comparable to control (Fig. 8a).

To determine whether SST interfere in Aβ-mediated changes in MMP activity, cell lysate prepared from control and treated cells was immunoblotted for MMP2 expression. MMP2 expression was increased in presence of Aβ in a dose-dependent manner and the increased level of MMP2 was ameliorated in presence of SST when used in combination with Aβ (Fig. 8b). Taken together, our results convincingly support the role of SST in the regulation of Aβ-induced changes in signal transduction pathways that might be associated with perturbed BBB function.

Discussion

The disintegration of BBB functionality with the progression of AD has been well documented; however, the molecular mechanisms involved in Aβ-induced damage to BBB remains elusive. In the present study, using hCMEC/D3 cells as an in vitro model of BBB, we demonstrate the expression and localization of TJPs, Aβ transporter LRP1 and RAGE and cell permeability in presence of Aβ. In addition, we also determined that the status of JNK phosphorylation and expression of MMP2 might play a crucial role in impairing BBB function

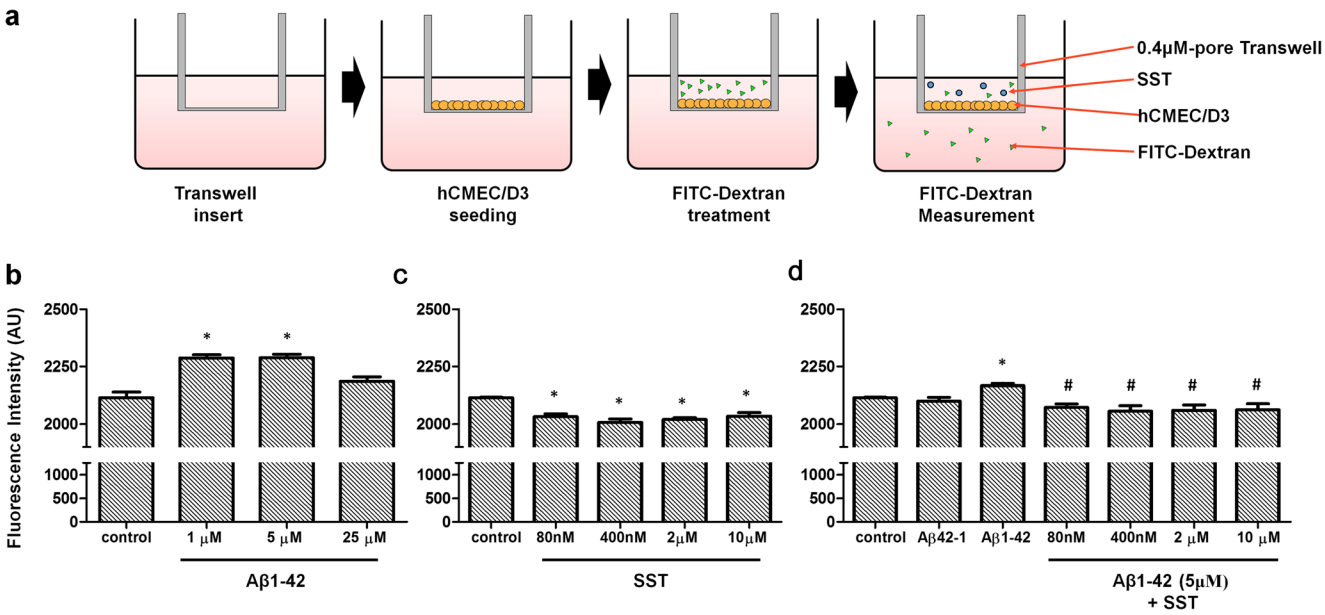

Fig. 6 Effects of Aβ and SST on hCMEC/D3 cell permeability. **a** Schematic representation of FITC-dextran permeability assay using transwell insert. **b** Following 1 and 5 μM treatment of Aβ, the FITC-dextran fluorescence in the basolateral chamber was significantly higher in comparison to control. In presence of higher concentration of Aβ (25 μM), the FITC-dextran intensity was enhanced, however, insignificantly. **c** SST exhibited inhibition of FITC-dextran fluorescence intensity in basolateral chamber compared to untreated group in all treatment conditions. **d** Aβ (5 μM) treatment resulted in significantly increased FITC-dextran fluorescence intensity. Note the significant inhibition of FITC-dextran in presence of SST and effective restoration of cell permeability. Aβ42-1 scrambled peptide was used as internal control. $*p < 0.05$ against control; $\#p < 0.05$ against Aβ1-42 treated alone

in Aβ-induced damage. Furthermore, the role of SST in abrogating the deleterious effect of Aβ in cell permeability and TJP organization at the cell-cell interaction has been studied. Our results uncovered an important role of SST in restoring the TJP distribution and expression of LRP1 and RAGE to regulate Aβ influx and efflux in hCMEC/D3 cells. Furthermore, the presence of SST suppressed the activation of JNK and expression of MMP2. Several studies have shown that SST improves cognitive function and memory recovery, work as a neurotrophic factor, improve the formation of synapses, and most importantly blocks the aggregation of Aβ [32, 40, 41]. Our results establish a functional association between the disruption of TJPs, changes in LRP1, and RAGE as well as signal transduction pathways in Aβ-induced toxicity model. To our knowledge, this is the first comprehensive description providing evidence in support of SST-mediated protection of BBB in Aβ-induced toxicity.

The release of pro-inflammatory cytokines such as IL-1β and TNF-α in AD patients leads to the loss of BBB functionality and increase barrier permeability. Aβ activates RAGE and inflammatory toll-like receptors, resulting in increased cytokine release [42–44]. In turn, the released cytokines form a positive feedback loop and promote further production of Aβ [45]. We recently reported that SST mediates suppression of LPS-induced release of TNF-α and IFN-γ and recovered ZO-1 expression at the cell surface in hCMEC/D3 cells. Also, SST effectively inhibits inflammation-induced damage to TJPs in vitro upon co-treatment with pro-inflammatory cytokines [33]. The anti-inflammatory effect of SST via SSTRs has been well established using *ko* mice [46–48]. Consistent with these observations, we have demonstrated that Aβ induces the release of IL-1β, which was significantly blunted in the presence of SST whereas SST release in response to Aβ tends to decrease albeit insignificantly. These results are consistent with previous studies suggesting that Aβ impaired SST processing from its precursor [49].

ZO-1, occludin, and claudin have been studied extensively for their prominent role in maintaining the paracellular integrity of BBB. Specifically, ZO-1 is a membrane protein at brain parenchyma localized to blood vessels forming an integral part of BBB [50]. Previous studies have reported that cytokines activate pro-inflammatory pathways in mouse brain endothelial cells leading to hyperphosphorylation of occludin, ZO-1, and claudin. This results in dissociation of these proteins from tight junction complexes, ultimately leading to the loss of barrier integrity and increased permeability [51, 52]. Most importantly, suppression of cytokines attenuates BBB permeability and restores inflammation-induced expression and organization of TJPs. Consistent with these findings, we observed a systematic increase of IL-1β in the presence of Aβ1-42, which led to a dose-dependent decrease in ZO-1 and occludin expression as well as disrupted organization. Importantly, such loss was effectively ameliorated in presence of SST.

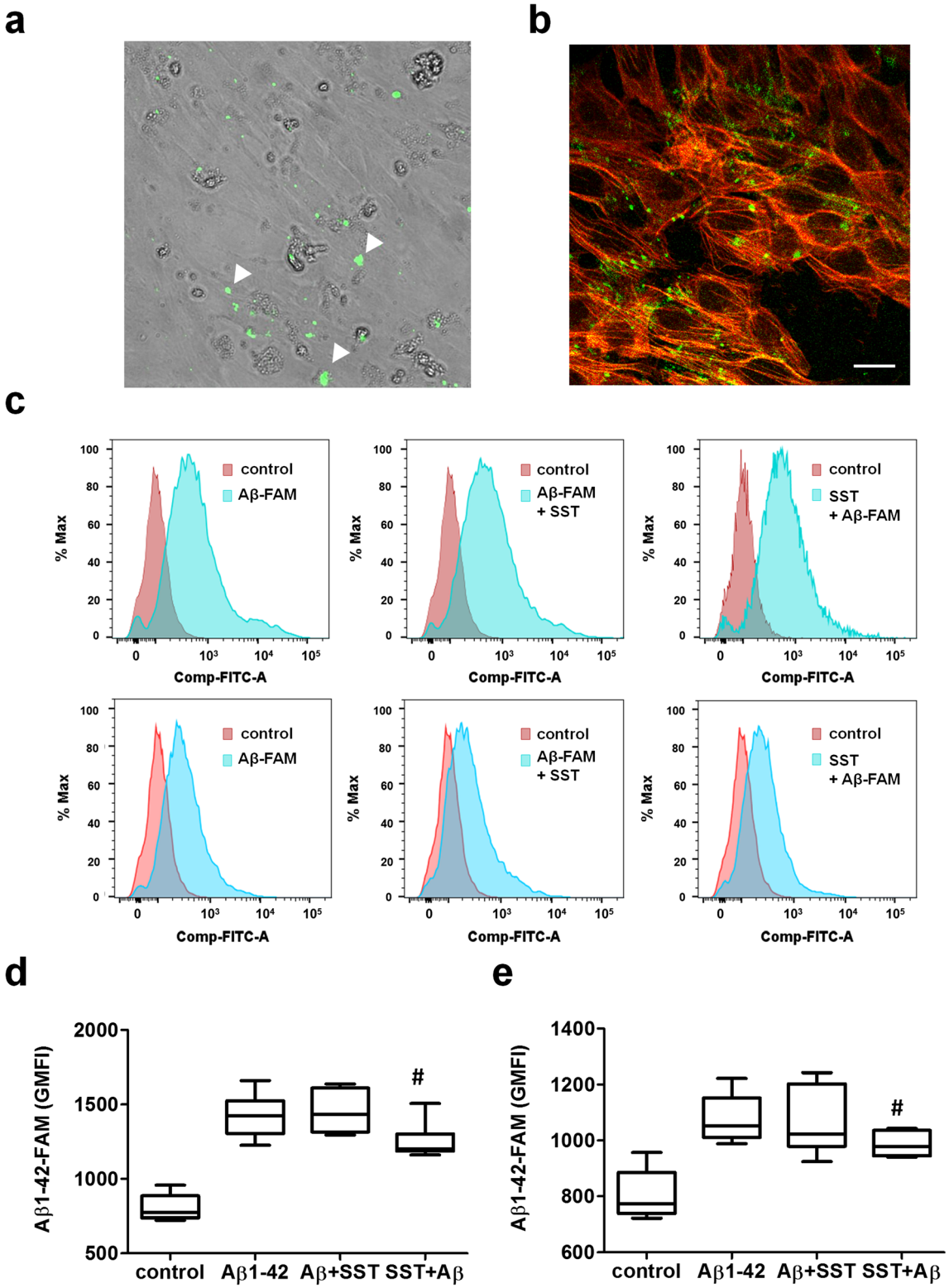

Fig. 7 Aβ uptake by BBB is regulated by SST. **a** Brightfield photograph of confluent hCMEC/D3 cells showing FAM-Aβ as bright green dots (arrowheads) following 10 min treatment. **b** Immunofluorescence staining of actin marker, phalloidin (red) with the intracellular uptake of FAM-Aβ (green). **c** Representative histogram of FAM-Aβ fluorescence intensity (blue) compared to negative control (red). Influx (upper panel) and efflux (bottom panel) is shown in three different conditions: FAM-Aβ treated alone (Aβ-FAM; left panel), FAM-Aβ co-treated with SST (Aβ-FAM + SST; middle panel), and cells treated with FAM-Aβ following 15-min treatment of SST (SST + Aβ-FAM; right panel). **d**, **e** Representative box blot displaying a summary of GMFI for each treatment group in influx (**d**) and efflux (**e**). #$p < 0.05$ against FAM-Aβ alone. These results are representative of six independent experiments and presented as mean ± SEM. *Scale bar* = 20 μm

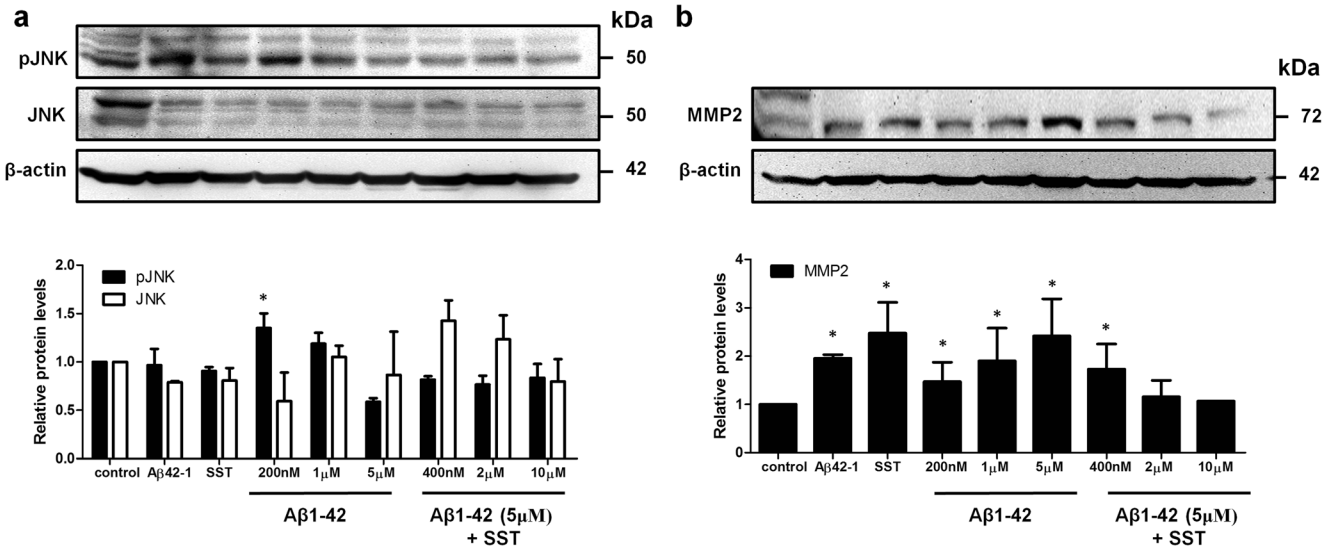

Fig. 8 SST inhibits Aβ-induced phosphorylation of JNK and expression of MMP2 in hCMEC/D3 cells. hCMEC/D3 cells were treated with increasing concentration of Aβ (200 nM–5 μM) alone or in combination with increasing concentration of SST (400 nM–10 μM) with Aβ (5 μM) for 24 h. Cell lysate prepared from control and treated cells was processed for immunoblot. **a** Aβ-mediated up-regulation of pJNK was inhibited in presence of SST. **b** Immunoblot showing increased expression of MMP2 in cells treated with Aβ. Note that the concentration-dependent inhibition of Aβ induced expression of MMP2. Histograms represent the densitometric analysis of expression when adjusted with β-actin as a loading control. Mean ± SEM from three independent experiments. *$p < 0.05$ against control

It is now well established that Aβ elicits significant changes in transporter proteins involved in clearance of Aβ and pathogenesis of AD involving LRP1 and RAGE as key modulators of such activity [39, 53, 54]. Previous in vitro study using hCMEC/D3 monolayer have shows decreased LRP1 while increased expression of RAGE upon treatment with Aβ1-40 or Aβ1-42 [55]. Recent studies have reported that LRP1 regulates matrix-degrading proteases such as MMPs and plasminogen activators (PAs) [56]. The clearance of MMP is primarily mediated via LRP-dependent endocytosis, where the decreased level of LRP1 in AD leads to accumulation of MMPs [57–59].

The role of pro-inflammatory cytokines IL-1β and TNFα in the regulation of MMP2 and its association with impaired BBB function in AD is well established [60–63]. In addition, MMP levels were found to be significantly higher in the hemorrhagic areas of the cerebral amyloid angiopathy brains, while MMP2 levels were also seen to be highly localized to astrocytes surrounding Aβ-affected vessels [64]. In *tg* mice model tg-SwDI, MMP2 levels were especially high in reactive astrocytes immediately surrounding Aβ plaques and cerebral microvascular fibrillar amyloid deposits [65]. Since hCMEC/D3 cells were cultured in the absence of astrocytes in the present study, changes seen in MMP2 expression might be associated with some other unknown mechanism. Subsequent studies using isolated rat brain microvessels have also shown decreased expression of claudin with increased expression of MMP2 and 9 in response to increasing concentration of Aβ1-40 [66]. Previous studies have also described that activation of JNK increases MMP expression [67]. Consistent with these observations, our results describe increased phosphorylation of JNK and MMP2 expression in presence of Aβ, which was inhibited in presence of SST. In support, the inhibition of JNK resulted in blockade of MMP2 expression implicating the direct role of JNK in regulation of MMP2 [67]. Taken together, the disturbed organization of TJPs and transporter proteins were effectively ameliorated in presence of SST, resulting in inhibition of Aβ uptake.

Our results revealed that at least in acute exposure to Aβ, the suppression of TJPs and changes in transporter proteins and signaling molecules are interconnected. With these observations, we speculate that anti-inflammatory effect of SST may alleviate the Aβ-induced pro-inflammatory cytokines, which in turn would prevent or inhibit the loss of integrity of BBB. We have convincingly demonstrated that Aβ-induced disruption in cell surface organization of TJPs and imbalance in LRP and RAGE expression in brain endothelial may be abrogated by SST. Most importantly, neprilysin (NEP) and insulin degrading enzyme (IDE) are the two most well-established enzymes identified to mediate proteolytic cleavage of Aβ [60–63, 68]. Interestingly, SST has also been identified as a potent activator of neprilysin, leading to increased catabolism of Aβ [32], further supporting the notion that SST plays a pivotal role in the homeostatic maintenance of BBB integrity.

With these observations, we hypothesize that gradual loss of SST in AD patients not only associated with a loss of memory and cognitive function but is also responsible for the disrupted and impaired BBB functionality and integrity. Whether this effect of SST on LRP1 and RAGE is mediated directly via activation of five different SST receptor subtypes

or indirectly through some other possible mechanism is not known and future studies are in progress in this direction. Taken together, these finding represents a novel insight into the role of SST in improving BBB permeability in Aβ-induced toxicity and strengthens SST as a potential target for treatment and prevention of AD. Collectively, our data indicate that SST may serve as a crucial signaling mechanism involved in the protection of BBB by blocking the JNK-MMP pathways.

Acknowledgements This work was funded by grants from Canadian Institute of Health Research (MOP 74465) and NSERC (402594-11, 16-05171) Canada to UK. SP is the recipient of CIHR Doctoral Fellowship. FACS study was aided by UBCFlow.

Author's Contribution This manuscript was written by SP and UK. Immunofluorescence colocalization, biochemical studies were done by SP and Western blot in part was done by RKS.

Compliance with Ethical Standards

Conflict of Interest The authors declare that they have no conflict of interest.

Abbreviations AD, Alzheimer's disease; Aβ, β-amyloid peptide; BBB, Blood-brain barrier; hCMEC/D3, Human cerebral microvascular endothelial cell line; CNS, Central nervous system; ECM, Extracellular matrix; FAM, Fluorescein amidite; IFN-γ, Interferon-γ; IL-1β, Interleukin 1β; JNK, c-Jun N-terminal kinases; *ko*, Knock out; LPS, Lipopolysaccharide; LRP, Lipoprotein receptor-related protein; MMP, Matrix metallopeptides; RAGE, Receptor for advanced glycation end products; SST, Somatostatin; SSTR, Somatostatin receptor; *tg*, Transgenic; TJP, Tight junction protein; TNF-α, Tumor necrosis factor-α; ZO, Zonula occluden

References

1. Selkoe DJ (2001) Alzheimer's disease: Genes, proteins, and therapy. Physiol Rev 81(2):741–766
2. Yankner BA (1996) Mechanisms of neuronal degeneration in Alzheimer's disease. Neuron 16(5):921–932
3. Grammas P (2011) Neurovascular dysfunction, inflammation and endothelial activation: Implications for the pathogenesis of Alzheimer's disease. J Neuroinflammation 8:26. https://doi.org/10.1186/1742-2094-8-26
4. Mhatre M, Nguyen A, Kashani S, Pham T, Adesina A, Grammas P (2004) Thrombin, a mediator of neurotoxicity and memory impairment. Neurobiol Aging 25(6):783–793. https://doi.org/10.1016/j.neurobiolaging.2003.07.007
5. Yin X, Wright J, Wall T, Grammas P (2010) Brain endothelial cells synthesize neurotoxic thrombin in Alzheimer's disease. Am J Pathol 176(4):1600–1606. https://doi.org/10.2353/ajpath.2010.090406
6. Kumar U (2005) Expression of somatostatin receptor subtypes (SSTR1-5) in Alzheimer's disease brain: An immunohistochemical analysis. Neuroscience 134(2):525–538. https://doi.org/10.1016/j.neuroscience.2005.04.001
7. Abbott NJ, Patabendige AA, Dolman DE, Yusof SR, Begley DJ (2010) Structure and function of the blood-brain barrier. Neurobiol Dis 37(1):13–25. https://doi.org/10.1016/j.nbd.2009.07.030
8. Begley DJ, Brightman MW (2003) Structural and functional aspects of the blood-brain barrier. Prog Drug Res Fortschr Arzneim Forsch Prog Rech Pharm 61:39–78
9. Hawkins BT, Davis TP (2005) The blood-brain barrier/neurovascular unit in health and disease. Pharmacol Rev 57(2):173–185. https://doi.org/10.1124/pr.57.2.4
10. Wolburg H, Noell S, Mack A, Wolburg-Buchholz K, Fallier-Becker P (2009) Brain endothelial cells and the glio-vascular complex. Cell Tissue Res 335(1):75–96. https://doi.org/10.1007/s00441-008-0658-9
11. Furuse M, Fujita K, Hiiragi T, Fujimoto K, Tsukita S (1998) Claudin-1 and -2: Novel integral membrane proteins localizing at tight junctions with no sequence similarity to occludin. J Cell Biol 141(7):1539–1550
12. Furuse M, Hirase T, Itoh M, Nagafuchi A, Yonemura S, Tsukita S, Tsukita S (1993) Occludin: A novel integral membrane protein localizing at tight junctions. J Cell Biol 123(6 Pt 2):1777–1788
13. Itoh M, Furuse M, Morita K, Kubota K, Saitou M, Tsukita S (1999) Direct binding of three tight junction-associated MAGUKs, ZO-1, ZO-2, and ZO-3, with the COOH termini of claudins. J Cell Biol 147(6):1351–1363
14. Tsukita S, Furuse M, Itoh M (1999) Structural and signalling molecules come together at tight junctions. Curr Opin Cell Biol 11(5):628–633
15. Eisenhauer PB, Johnson RJ, Wells JM, Davies TA, Fine RE (2000) Toxicity of various amyloid beta peptide species in cultured human blood-brain barrier endothelial cells: Increased toxicity of dutch-type mutant. J Neurosci Res 60(6):804–810. https://doi.org/10.1002/1097-4547(20000615)60:6<804::aid-jnr13>3.0.co;2-1
16. Kalaria RN (2010) Vascular basis for brain degeneration: Faltering controls and risk factors for dementia. Nutr Rev 68(Suppl 2):S74–S87. https://doi.org/10.1111/j.1753-4887.2010.00352.x
17. Zlokovic BV (2008) The blood-brain barrier in health and chronic neurodegenerative disorders. Neuron 57(2):178–201. https://doi.org/10.1016/j.neuron.2008.01.003
18. Huttunen HJ, Kuja-Panula J, Sorci G, Agneletti AL, Donato R, Rauvala H (2000) Coregulation of neurite outgrowth and cell survival by amphoterin and S100 proteins through receptor for advanced glycation end products (RAGE) activation. J Biol Chem 275(51):40096–40105. https://doi.org/10.1074/jbc.M006993200
19. Kanekiyo T, Cirrito JR, Liu CC, Shinohara M, Li J, Schuler DR, Shinohara M, Holtzman DM et al (2013) Neuronal clearance of amyloid-beta by endocytic receptor LRP1. J Neurosci 33(49):19276–19283. https://doi.org/10.1523/jneurosci.3487-13.2013
20. Kook SY, Seok Hong H, Moon M, Mook-Jung I (2013) Disruption of blood-brain barrier in Alzheimer disease pathogenesis. Tissue Barriers 1(2):e23993. https://doi.org/10.4161/tisb.23993
21. Chen F, Ohashi N, Li W, Eckman C, Nguyen JH (2009) Disruptions of occludin and claudin-5 in brain endothelial cells in vitro and in brains of mice with acute liver failure. Hepatology (Baltimore, Md) 50(6):1914–1923. https://doi.org/10.1002/hep.23203
22. Gu Z, Cui J, Brown S, Fridman R, Mobashery S, Strongin AY, Lipton SA (2005) A highly specific inhibitor of matrix metalloproteinase-9 rescues laminin from proteolysis and neurons from apoptosis in transient focal cerebral ischemia. J Neurosci 25(27):6401–6408. https://doi.org/10.1523/jneurosci.1563-05.2005
23. Dhanda S, Sandhir R (2017) Blood-brain barrier permeability is exacerbated in experimental model of hepatic encephalopathy via MMP-9 activation and downregulation of tight junction proteins. Mol Neurobiol. https://doi.org/10.1007/s12035-017-0521-7
24. Beal MF (1990) Somatostatin in neurodegenerative illnesses. Metab Clin Exp 39(9 Suppl 2):116–119
25. Binaschi A, Bregola G, Simonato M (2003) On the role of somatostatin in seizure control: Clues from the hippocampus. Rev Neurosci 14(3):285–301

26. Epelbaum J, Dournaud P, Fodor M, Viollet C (1994) The neurobiology of somatostatin. Crit Rev Neurobiol 8(1–2):25–44
27. Fox L, Alford M, Achim C, Mallory M, Masliah E (1997) Neurodegeneration of somatostatin-immunoreactive neurons in HIV encephalitis. J Neuropathol Exp Neurol 56(4):360–368
28. Davies P, Katzman R, Terry RD (1980) Reduced somatostatin-like immunoreactivity in cerebral cortex from cases of Alzheimer disease and Alzheimer senile dementa. Nature 288(5788):279–280
29. Kowall NW, Beal MF (1988) Cortical somatostatin, neuropeptide Y, and NADPH diaphorase neurons: Normal anatomy and alterations in Alzheimer's disease. Ann Neurol 23(2):105–114. https://doi.org/10.1002/ana.410230202
30. Beal MF, Mazurek MF, Tran VT, Chattha G, Bird ED, Martin JB (1985) Reduced numbers of somatostatin receptors in the cerebral cortex in Alzheimer's disease. Science (New York, NY) 229(4710): 289–291
31. Geci C, How J, Alturaihi H, Kumar U (2007) Beta-amyloid increases somatostatin expression in cultured cortical neurons. J Neurochem 101(3):664–673. https://doi.org/10.1111/j.1471-4159.2006.04415.x
32. Saito T, Iwata N, Tsubuki S, Takaki Y, Takano J, Huang SM, Suemoto T, Higuchi M et al (2005) Somatostatin regulates brain amyloid beta peptide Abeta42 through modulation of proteolytic degradation. Nat Med 11(4):434–439. https://doi.org/10.1038/nm1206
33. Basivireddy J, Somvanshi RK, Romero IA, Weksler BB, Couraud PO, Oger J, Kumar U (2013) Somatostatin preserved blood brain barrier against cytokine induced alterations: Possible role in multiple sclerosis. Biochem Pharmacol 86(4):497–507. https://doi.org/10.1016/j.bcp.2013.06.001
34. Adori C, Gluck L, Barde S, Yoshitake T, Kovacs GG, Mulder J, Magloczky Z, Havas L et al (2015) Critical role of somatostatin receptor 2 in the vulnerability of the central noradrenergic system: New aspects on Alzheimer's disease. Acta Neuropathol 129(4): 541–563. https://doi.org/10.1007/s00401-015-1394-3
35. Weksler BB, Subileau EA, Perriere N, Charneau P, Holloway K, Leveque M, Tricoire-Leignel H, Nicotra A et al (2005) Blood-brain barrier-specific properties of a human adult brain endothelial cell line. FASEB J 19(13):1872–1874. https://doi.org/10.1096/fj.04-3458fje
36. Alemi M, Gaiteiro C, Ribeiro CA, Santos LM, Gomes JR, Oliveira SM, Couraud PO, Weksler B et al (2016) Transthyretin participates in beta-amyloid transport from the brain to the liver–involvement of the low-density lipoprotein receptor-related protein 1? Sci Rep 6: 20164. https://doi.org/10.1038/srep20164
37. Loo DT, Copani A, Pike CJ, Whittemore ER, Walencewicz AJ, Cotman CW (1993) Apoptosis is induced by beta-amyloid in cultured central nervous system neurons. Proc Natl Acad Sci U S A 90(17):7951–7955
38. Deane R, Du Yan S, Submamaryan RK, LaRue B, Jovanovic S, Hogg E, Welch D, Manness L et al (2003) RAGE mediates amyloid-beta peptide transport across the blood-brain barrier and accumulation in brain. Nat Med 9(7):907–913. https://doi.org/10.1038/nm890
39. Deane R, Sagare A, Zlokovic BV (2008) The role of the cell surface LRP and soluble LRP in blood-brain barrier Abeta clearance in Alzheimer's disease. Curr Pharm Des 14(16):1601–1605
40. Liguz-Lecznar M, Urban-Ciecko J, Kossut M (2016) Somatostatin and somatostatin-containing neurons in shaping neuronal activity and plasticity. Front Neural Circuits 10:48. https://doi.org/10.3389/fncir.2016.00048
41. Matsuoka N, Maeda N, Yamaguchi I, Satoh M (1994) Possible involvement of brain somatostatin in the memory formation of rats and the cognitive enhancing action of FR121196 in passive avoidance task. Brain Res 642(1–2):11–19
42. Abbott NJ (2000) Inflammatory mediators and modulation of blood-brain barrier permeability. Cell Mol Neurobiol 20(2):131–147
43. Ramasamy R, Yan SF, Schmidt AM (2009) RAGE: Therapeutic target and biomarker of the inflammatory response–the evidence mounts. J Leukoc Biol 86(3):505–512. https://doi.org/10.1189/jlb.0409230
44. Reed-Geaghan EG, Savage JC, Hise AG, Landreth GE (2009) CD14 and toll-like receptors 2 and 4 are required for fibrillar a{beta}-stimulated microglial activation. J Neurosci 29(38):11982–11992. https://doi.org/10.1523/jneurosci.3158-09.2009
45. Smith DG, Cappai R, Barnham KJ (2007) The redox chemistry of the Alzheimer's disease amyloid beta peptide. Biochim Biophys Acta 1768(8):1976–1990. https://doi.org/10.1016/j.bbamem.2007.02.002
46. Green PG, Basbaum AI, Levine JD (1992) Sensory neuropeptide interactions in the production of plasma extravasation in the rat. Neuroscience 50(3):745–749
47. Szolcsanyi J, Helyes Z, Oroszi G, Nemeth J, Pinter E (1998) Release of somatostatin and its role in the mediation of the anti-inflammatory effect induced by antidromic stimulation of sensory fibres of rat sciatic nerve. Br J Pharmacol 123(5):936–942. https://doi.org/10.1038/sj.bjp.0701685
48. Szolcsanyi J, Pinter E, Helyes Z, Oroszi G, Nemeth J (1998) Systemic anti-inflammatory effect induced by counter-irritation through a local release of somatostatin from nociceptors. Br J Pharmacol 125(4):916–922. https://doi.org/10.1038/sj.bjp.0702144
49. Epelbaum J, Guillou JL, Gastambide F, Hoyer D, Duron E, Viollet C (2009) Somatostatin, Alzheimer's disease and cognition: An old story coming of age? Prog Neurobiol 89(2):153–161. https://doi.org/10.1016/j.pneurobio.2009.07.002
50. Tornavaca O, Chia M, Dufton N, Almagro LO, Conway DE, Randi AM, Schwartz MA, Matter K et al (2015) ZO-1 controls endothelial adherens junctions, cell-cell tension, angiogenesis, and barrier formation. J Cell Biol 208(6):821–838. https://doi.org/10.1083/jcb.201404140
51. Stamatovic SM, Dimitrijevic OB, Keep RF, Andjelkovic AV (2006) Protein kinase Calpha-RhoA cross-talk in CCL2-induced alterations in brain endothelial permeability. J Biol Chem 281(13): 8379–8388. https://doi.org/10.1074/jbc.M513122200
52. Stamatovic SM, Keep RF, Kunkel SL, Andjelkovic AV (2003) Potential role of MCP-1 in endothelial cell tight junction 'opening': Signaling via rho and rho kinase. J Cell Sci 116(Pt 22):4615–4628. https://doi.org/10.1242/jcs.00755
53. Cirrito JR, Deane R, Fagan AM, Spinner ML, Parsadanian M, Finn MB, Jiang H, Prior JL et al (2005) P-glycoprotein deficiency at the blood-brain barrier increases amyloid-beta deposition in an Alzheimer disease mouse model. J Clin Invest 115(11):3285–3290. https://doi.org/10.1172/jci25247
54. Qosa H, Abuznait AH, Hill RA, Kaddoumi A (2012) Enhanced brain amyloid-beta clearance by rifampicin and caffeine as a possible protective mechanism against Alzheimer's disease. J Alzheimers Dis 31(1):151–165. https://doi.org/10.3233/jad-2012-120319
55. Qosa H, LeVine H 3rd, Keller JN, Kaddoumi A (2014) Mixed oligomers and monomeric amyloid-beta disrupts endothelial cells integrity and reduces monomeric amyloid-beta transport across hCMEC/D3 cell line as an in vitro blood-brain barrier model. Biochim Biophys Acta 1842(9):1806–1815. https://doi.org/10.1016/j.bbadis.2014.06.029
56. Etique N, Verzeaux L, Dedieu S, Emonard H (2013) LRP-1: A checkpoint for the extracellular matrix proteolysis. Biomed Res Int 2013:152163–152167. https://doi.org/10.1155/2013/152163
57. Barmina OY, Walling HW, Fiacco GJ, Freije JM, Lopez-Otin C, Jeffrey JJ, Partridge NC (1999) Collagenase-3 binds to a specific receptor and requires the low density lipoprotein receptor-related protein for internalization. J Biol Chem 274(42):30087–30093

58. Van den Steen PE, Van Aelst I, Hvidberg V, Piccard H, Fiten P, Jacobsen C, Moestrup SK, Fry S et al (2006) The hemopexin and O-glycosylated domains tune gelatinase B/MMP-9 bioavailability via inhibition and binding to cargo receptors. J Biol Chem 281(27): 18626–18637. https://doi.org/10.1074/jbc.M512308200
59. Yang Z, Strickland DK, Bornstein P (2001) Extracellular matrix metalloproteinase 2 levels are regulated by the low density lipoprotein-related scavenger receptor and thrombospondin 2. J Biol Chem 276(11):8403–8408. https://doi.org/10.1074/jbc.M008925200
60. Chen KL, Wang SS, Yang YY, Yuan RY, Chen RM, Hu CJ (2009) The epigenetic effects of amyloid-beta(1-40) on global DNA and neprilysin genes in murine cerebral endothelial cells. Biochem Biophys Res Commun 378(1):57–61. https://doi.org/10.1016/j.bbrc.2008.10.173
61. Gao W, Eisenhauer PB, Conn K, Lynch JA, Wells JM, Ullman MD, McKee A, Thatte HS et al (2004) Insulin degrading enzyme is expressed in the human cerebrovascular endothelium and in cultured human cerebrovascular endothelial cells. Neurosci Lett 371(1):6–11. https://doi.org/10.1016/j.neulet.2004.07.034
62. Iwata N, Tsubuki S, Takaki Y, Watanabe K, Sekiguchi M, Hosoki E, Kawashima-Morishima M, Lee HJ et al (2000) Identification of the major Abeta1-42-degrading catabolic pathway in brain parenchyma: Suppression leads to biochemical and pathological deposition. Nat Med 6(2):143–150. https://doi.org/10.1038/72237
63. Lynch JA, George AM, Eisenhauer PB, Conn K, Gao W, Carreras I, Wells JM, McKee A et al (2006) Insulin degrading enzyme is localized predominantly at the cell surface of polarized and unpolarized human cerebrovascular endothelial cell cultures. J Neurosci Res 83(7):1262–1270. https://doi.org/10.1002/jnr.20809
64. Hernandez-Guillamon M, Martinez-Saez E, Delgado P, Domingues-Montanari S, Boada C, Penalba A, Boada M, Pagola J et al (2012) MMP-2/MMP-9 plasma level and brain expression in cerebral amyloid angiopathy-associated hemorrhagic stroke. Brain Pathol (Zurich, Switzerland) 22(2):133–141. https://doi.org/10.1111/j.1750-3639.2011.00512.x
65. Yin KJ, Cirrito JR, Yan P, Hu X, Xiao Q, Pan X, Bateman R, Song H et al (2006) Matrix metalloproteinases expressed by astrocytes mediate extracellular amyloid-beta peptide catabolism. J Neurosci 26(43):10939–10948. https://doi.org/10.1523/jneurosci.2085-06.2006
66. Hartz AM, Bauer B, Soldner EL, Wolf A, Boy S, Backhaus R, Mihaljevic I, Bogdahn U et al (2012) Amyloid-beta contributes to blood-brain barrier leakage in transgenic human amyloid precursor protein mice and in humans with cerebral amyloid angiopathy. Stroke 43(2):514–523. https://doi.org/10.1161/strokeaha.111.627562
67. Fromigue O, Hamidouche Z, Marie PJ (2008) Blockade of the RhoA-JNK-c-Jun-MMP2 cascade by atorvastatin reduces osteosarcoma cell invasion. J Biol Chem 283(45):30549–30556. https://doi.org/10.1074/jbc.M801436200
68. Qosa H, Abuasal BS, Romero IA, Weksler B, Couraud PO, Keller JN, Kaddoumi A (2014) Differences in amyloid-beta clearance across mouse and human blood-brain barrier models: Kinetic analysis and mechanistic modeling. Neuropharmacology 79:668–678. https://doi.org/10.1016/j.neuropharm.2014.01.023